

# Using wavelength and slope to infer the historical origin of semiarid vegetation bands

Jonathan A. Sherratt<sup>1</sup>

Department of Mathematics and Maxwell Institute for Mathematical Sciences, Heriot-Watt University, Edinburgh EH14 4AS, United Kingdom

Edited by Simon A. Levin, Princeton University, Princeton, NJ, and approved February 24, 2015 (received for review October 21, 2014)

Landscape-scale patterns of vegetation occur worldwide at interfaces between semiarid and arid climates. They are important as potential indicators of climate change and imminent regime shifts and are widely thought to arise from positive feedback between vegetation and infiltration of rainwater. On gentle slopes the typical pattern form is bands (stripes), oriented parallel to the contours, and their wavelength is probably the most accessible statistic for vegetation patterns. Recent field studies have found an inverse correlation between pattern wavelength and slope, in apparent contradiction with the predictions of mathematical models. Here I show that this “contradiction” is based on a flawed approach to calculating the wavelength in models. When pattern generation is considered in detail, the theory is fully consistent with empirical results. For realistic parameters, degradation of uniform vegetation generates patterns whose wavelength increases with slope, whereas colonization of bare ground gives the opposite trend. Therefore, the empirical finding of an inverse relationship can be used, in conjunction with climate records, to infer the historical origin of the patterns. Specifically, for the African Sahel my results suggest that banded vegetation originated by the colonization of bare ground during circa 1760–1790 or since circa 1850.

banded vegetation | pattern formation | mathematical modeling

Landscape-scale patterns of vegetation occur worldwide at interfaces between semiarid and arid climates (1). They are important as potential indicators of climate change and imminent regime shifts (2, 3). Although other mechanisms have been suggested (4, 5), the patterns are widely thought to arise from positive feedback between vegetation and infiltration of rainwater (3, 6). Local increases in vegetation density cause greater infiltration, which promotes further growth, whereas rain falling on sparsely vegetated areas tends to run off to adjacent vegetated patches. On gentle slopes, the typical pattern form is bands (stripes), oriented parallel to the contours (6, 7), and their wavelength is probably the most accessible statistic for vegetation patterns, because it can be estimated from remotely captured images. The database of wavelengths is extensive, and some studies also record slope gradient. In 1999 Eddy et al. (8) compiled various older data of this type. Both this and a parallel study by d’Herbès et al. (9) showed an inverse relationship: longer wavelengths tend to occur on shallower slopes. The inferred relationship was not very strong because the data came from a variety of locations and involved a range of vegetation types, with relatively few data points from any one study. However, an inverse relationship between slope and wavelength has also been found in three recent detailed studies, of the African Sahel (10) and southwest United States (5, 11).

The dependence of wavelength on slope can also be investigated using mathematical models based on water redistribution. Those studies that have done this report the opposite trend: Wavelength increases with slope (11, 12). This apparent contradiction has led to questioning of the mechanistic basis for vegetation patterns (5, 11). However, previous studies have made the conventional assumption that patterns arise from preexisting unstable uniformly vegetated states. I will argue that this assumption, and hence the contradiction, are invalid. Further I will

show that detailed consideration of pattern generation mechanisms in mathematical models can reproduce the observed inverse relationship, showing that this relationship is entirely consistent with the water redistribution mechanism. Moreover my approach gives valuable insights into the historical origin of these patterns.

## Mathematical Modeling of Semiarid Vegetation

Mathematical models play a key role in understanding arid ecosystems, and a wide variety of models have been proposed over the last two decades, ranging from detailed multiscale representations of soil–water dynamics (13) to simple models of key underlying mechanisms (14–18). I will investigate the extent to which qualitative trends in wavelength apply irrespective of parameter values. This requires comprehensive scans across parameter space, which is only possible for very simple models. Therefore, I use the Klausmeier model (14):

$$\begin{aligned} \frac{\partial u}{\partial t} &= \overbrace{wu^2}^{\text{plant growth}} - \overbrace{Bu}^{\text{plant loss}} + \overbrace{\partial^2 u / \partial x^2}^{\text{plant dispersal}} \\ \frac{\partial w}{\partial t} &= \underbrace{A}_{\text{average rainfall}} - \underbrace{w}_{\text{evaporation}} - \underbrace{wu^2}_{\text{uptake by plants}} + \underbrace{\nu \partial w / \partial x}_{\text{flow downhill}} + \underbrace{D \partial^2 w / \partial x^2}_{\text{diffusion of water}}. \end{aligned} \quad [1]$$

In this nondimensionalized form of the model equations (12, 14)  $u(x, t)$  and  $w(x, t)$  denote vegetation biomass and water density, respectively,  $t$  denotes time, and distance  $x$  is measured in the uphill direction. I assume a uniform slope and throughout I will consider behavior in one spatial dimension, which is sufficient for banded patterns.

Eq. 1 is one of the earliest and simplest models for vegetation patterning, and remains in widespread use (19–23). Crucially, there are only four dimensionless parameters, which makes comprehensive scans of parameter space feasible. The key driver

## Significance

Self-organized vegetation patterns are a characteristic feature of semiarid regions. On gentle slopes banded patterns (stripes) are typical, and their wavelength is probably the most accessible statistic for patterned vegetation. Recent data show that on steeper slopes wavelengths are usually shorter, contradicting previous predictions of mathematical models. I resolve this “contradiction” by a detailed theoretical study of pattern generation. Moreover I show that the wavelength–slope relationship has a wholly unexpected predictive power, enabling one to infer whether the patterns arose from degradation of uniform vegetation or colonization of bare ground. When combined with climate records, this gives valuable insights into the historical origin of the patterns.

Author contributions: J.A.S. designed research, performed research, analyzed data, and wrote the paper.

The author declares no conflict of interest.

This article is a PNAS Direct Submission.

<sup>1</sup>Email: j.a.sherratt@hw.ac.uk.

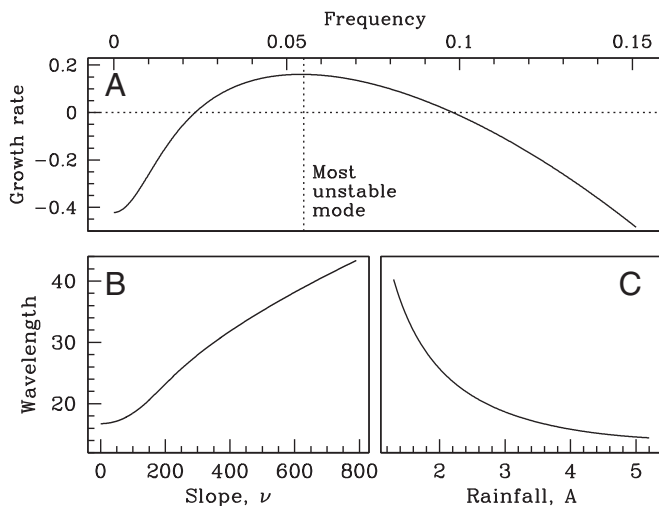


**Fig. 1.** Pattern generation from preexisting unstable vegetation, with rainfall fixed. (A) The expected wavelength is determined by the most unstable mode, and is (B) positively correlated with slope and (C) negatively correlated with rainfall. Parameters: (A–C)  $B = 0.45$ ,  $D = 500$ ; (A and B)  $A = 2$ ; (A and C)  $\nu = 250$ .

of pattern formation in [1] is the assumption that the per capita specific water uptake is proportional to biomass density. This is based on extensive empirical evidence that in semiarid environments, rainwater infiltration is positively correlated with vegetation cover (24, 25), due to increasing levels of organic matter in the soil, and to the presence of root networks (26, 27). The parameter  $A$  represents an average rate of rainfall, which typically occurs in discrete storm events in semiarid regions (28, 29). The plant loss term includes both natural death and the effects of any herbivory. Diffusion is used to model plant dispersal in the interests of mathematical simplicity; some subsequent models have used instead a nonlocal dispersal term (30, 31). Klausmeier's original formulation (14) did not include water diffusion but this has been added by a number of subsequent authors (20–23). Because  $D$  will typically be much larger than the (dimensionless) plant dispersal coefficient of 1, this additional term tends to enhance the pattern forming potential of the model.

When rainfall  $A$  is large, [1] predicts a stable uniformly vegetated state. As rainfall is decreased, this becomes unstable, giving spatial patterns (12, 32). To investigate the wavelengths of such patterns, one considers disturbances to the uniform vegetated state with a particular spatial frequency and calculates their growth (or decay) rate. One particular frequency will give the largest growth rate; this is the “most unstable mode” (Fig. 1A), from which one can calculate the expected pattern wavelength (Methods). Intuitively, there is a range of possible vegetation band widths and interband spacings, but one of these (the most unstable mode) becomes established most quickly, and then suppresses the others.

I found that whenever the rainfall  $A$  is below the critical value for patterns, the expected wavelength is positively correlated with slope (Fig. 1B and Methods). The same trend has been found in much less systematic studies of other models (11, 12). Moreover it is expected, because of the increased run-off on steeper gradients. However, this positive correlation is the opposite of the wavelength–slope relationship found empirically (5, 8–11).

### Pattern Generation from Uniform Vegetation

Calculation of wavelength using the most unstable mode assumes that patterns arise via disturbance of a state that is uniformly vegetated but unstable. This raises the very natural question of how the system arrived at an unstable state in the first place. By definition, unstable states will disappear in response to the small perturbations that are inherent to any biological process. Therefore, in a real system the key issue is how and when a state

changes from stable to unstable. Historically, the first theoretical work on biological pattern formation concerned embryonic development. There a stability change might result from a particular gene being expressed during development (e.g., ref. 33), which would correspond to an abrupt change in the parameter values in a mathematical model. Alternatively a uniform state might be stable in an embryo that is too small to permit the destabilizing frequencies, but becomes unstable as the embryo grows (e.g., ref. 34). Such mechanisms can generate any unstable uniform state, and thence patterns. However, for semiarid vegetation a uniform state can only lose stability via changes in environmental parameters such as rainfall (35, 36), which are inherently gradual. Therefore, marginally stable uniform states can occur, but those that are fully unstable cannot.

It follows that the most unstable mode approach to the calculation of pattern wavelength and the resultant contradiction are not relevant to banded vegetation. Nevertheless prediction of pattern wavelength is possible. Studies of both [1] and other models for semiarid vegetation have shown that as environmental parameters are gradually changed, the wavelength of banded vegetation patterns remains constant (19, 23, 37, 38) (Fig. 2). The patterns do alter of course: for example, a decrease in rainfall causes both net biomass and band:interband ratio to decrease, but the wavelength is unchanged. Intuitively, lower (higher) rainfall leads to retraction (expansion) of the edges of each vegetation band, so that patterns change without a change in wavelength. Eventually rainfall levels can become too low (high) to sustain a pattern with that wavelength. Models then predict that the pattern breaks down and reforms with a longer (shorter) wavelength (Fig. 2); the occurrence of such transitions can be predicted via the patterns crossing the “stability boundary” (19, 23, 38) (Fig. 2).

Wavelength persistence implies that the key to its prediction lies in calculating it when patterns are first established, which can happen in two ways. Patterns might develop from uniform vegetation when changes in an environmental parameter such as rainfall cause that uniform state to become unstable, implying pattern onset via a marginally stable state. Alternatively patterns

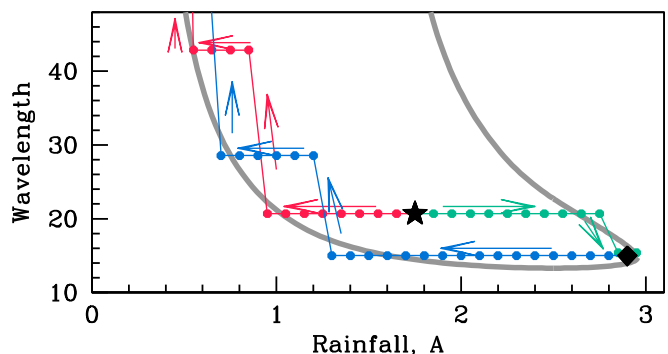


**Fig. 2.** Pattern wavelength remains constant as rainfall is gradually changed. The colored lines and filled circles show pattern wavelength in simulations of [1] when rainfall  $A$  is increased or decreased by 0.1 every 500 time units. Results of three long simulations are shown, each in a different color: decreasing rainfall starting from the pattern generated by the degradation of uniform vegetation ( $\blacklozenge$ ), and increasing and decreasing rainfall starting from the pattern generated by the colonization of bare ground ( $\star$ ). In all three cases wavelength remains constant until the pattern falls outside the stability boundary (thick gray line); at that point the pattern breaks down and reforms with a new wavelength. For the simulation shown in green, patterns are replaced by (stable) uniform vegetation when rainfall  $A$  is increased above 3. Note that the parameter region inside the stability boundary is sometimes known as the “Busse balloon” (23). The equations were solved on a domain of length 600 with periodic boundary conditions, and the wavelengths were recorded immediately before each change in rainfall. Parameters:  $B = 0.45$ ,  $D = 500$ ,  $\nu = 60$ ; these imply that colonization of bare ground is initiated at  $A \approx 1.75$ .

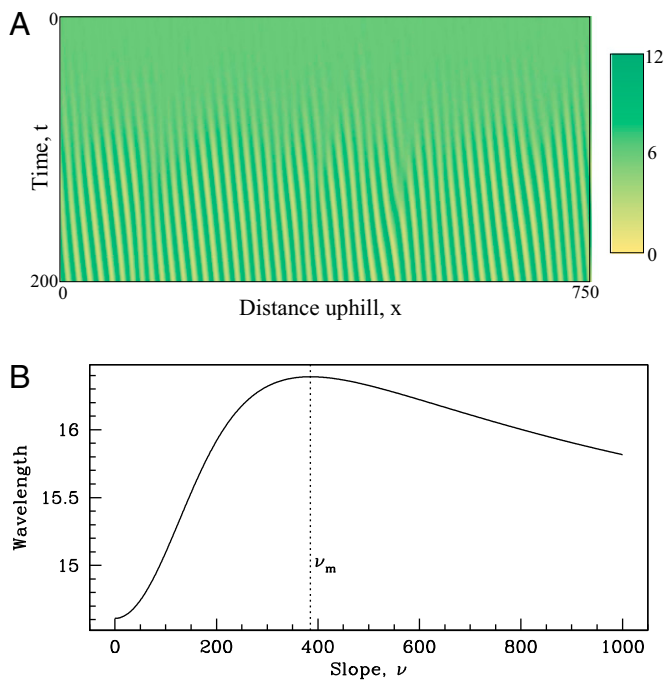


**Fig. 3.** Pattern generation by degradation of uniform vegetation. (A) An example of such pattern generation. (B) Wavelength varies nonmonotonically with slope. Note that in *B* rainfall is varied with slope to give the pattern onset point; this contrasts with Fig. 1*B*, in which the plotted wavelength corresponds to the most unstable frequency at a fixed rainfall level. Parameters:  $B = 0.45$ ,  $D = 500$  and (A)  $A = 2.8$ ,  $\nu = 100$ . The initial conditions in *A* are small random perturbations to the uniformly vegetated state, and the value of  $A$  is a little below the pattern onset point of 3.08. The colors in *A* indicate vegetation biomass  $u$  as shown in the scale bar.

might arise through a quite different route that has no analog in embryonic pattern formation: colonization of bare ground (36). The two starting patterns used in Fig. 2 are those generated by these two initiation mechanisms: in both cases pattern wavelength remains constant over a wide range of rainfall levels, and is determined at the initial formation of the pattern.

For patterns arising from degradation of uniform vegetation, i.e., from a marginally stable uniform state (e.g., Fig. 3*A*), the wavelength–slope relationship is the result of a trade-off. The wavelength corresponding to the most unstable mode increases with slope. However, steeper slopes facilitate patterning, so that pattern onset occurs at higher rainfall levels, and this tends to decrease the wavelength (Fig. 1*C*). One consequence of this is that the overall variation in wavelength with slope is relatively small, e.g., 11% in Fig. 3*B* compared with 88% in Fig. 1*B*. Moreover, the resulting wavelength–slope relationship is non-monotonic (Fig. 3*B*), as found previously by Ursino (20). Pattern wavelength increases with slope when this is small, reaches a maximum at  $\nu = \nu_m$ , say, and then decreases as slope is increased further. Intuitively, on shallow slopes a change in gradient is very significant and dominates the effect of the change in rainfall level required to give the pattern onset point; the reverse applies on steeper slopes. Note that in Fig. 1*B* rainfall is fixed, and the plotted wavelength corresponds to the most unstable mode, which is the expected pattern. In contrast, in Fig. 3*B* rainfall varies with slope to give the pattern onset point. I found that the qualitative form of Fig. 3*B* applies for all relevant parameters. Although these results appear to provide a potential explanation for the empirically observed negative correlation between wavelength and slope, all parameter estimates in the literature actually give  $\nu < \nu_m$  (Methods and Fig. 4). Thus, for realistic parameters the wavelength of patterns generated by degradation of uniform vegetation is positively correlated with slope.

### Pattern Generation from Bare Ground

I now consider banded patterns initiated by the colonization of bare ground. Mathematically this is much more difficult because it cannot be studied via small perturbations to a uniform state: it is a fundamentally nonlinear problem. In addition to the uniformly vegetated state, [1] also has a uniform unvegetated state that is stable to small perturbations for all parameter sets. Intuitively one expects that when rainfall is sufficiently high, a localized introduction of plants will invade and colonize this bare ground state, and I confirmed this in simulations of [1]. Such an invasion involves a transition between two locally stable states, a situation that has been well studied for many biological applications (39, 40; ref. 41, chap. 5). The propagation direction depends on the details of the nonlinear terms (42, 43): intuitively, a smaller proportion of uniform initial solutions tends to one of the stable states than the other, and it is that state that is invaded. Formulas for the invasion speed can only be calculated in the very simplest cases, and I studied colonization for [1] using simulations.

I found that in comparison with flat terrain, vegetation has a greater tendency to expand in an uphill direction. Intuitively this is because the downhill flow of water facilitates vegetation growth at the edge of the invading front. Similarly, downhill spread is impeded in comparison with flat ground. These findings are reflected by the empirical observation of higher seedling densities on the uphill edge of vegetation patches, and higher levels of plant death on the downhill edges (44–46). Therefore, at low levels of rainfall, both edges of a localized vegetation patch on a slope move uphill (Fig. 5*A*); the downhill edge moves uphill because plant loss exceeds growth. To colonize bare ground, the downhill edge of a vegetation patch must invade in the downhill direction, which occurs only for rainfall levels above a critical minimum (Fig. 5*B*). After a drought during which vegetation has died out, recolonization will commence when rainfall increases to this critical level, establishing a particular pattern wavelength which will then persist following subsequent moderate variations in rainfall.

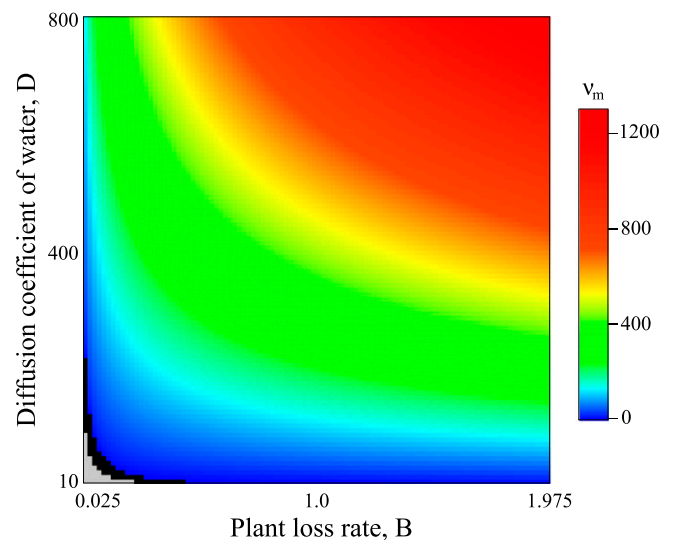


**Fig. 4.** Dependence of the critical slope gradient  $\nu_m$  on plant loss  $B$  and water diffusion  $D$ . For patterns generated by degradation of uniform vegetation, wavelength is negatively (positively) correlated with slope for  $\nu$  greater (less) than  $\nu_m$ . The scale bar shows the color scale for  $\nu_m$ , which is deliberately skewed to give greater visual clarity. In the gray and black regions of the parameter plane (lower left-hand corner), wavelength always decreases with  $\nu$ . In the black region patterns exist for all  $\nu \geq 0$ , whereas in the gray region patterns only exist for  $\nu$  greater than some nonzero minimum, so that there are no patterns on flat ground. The gray and black regions are separated by the curve  $BD = 2$ , which is the threshold for stability of  $(u_s, w_s)$  when  $A = 2B$ .

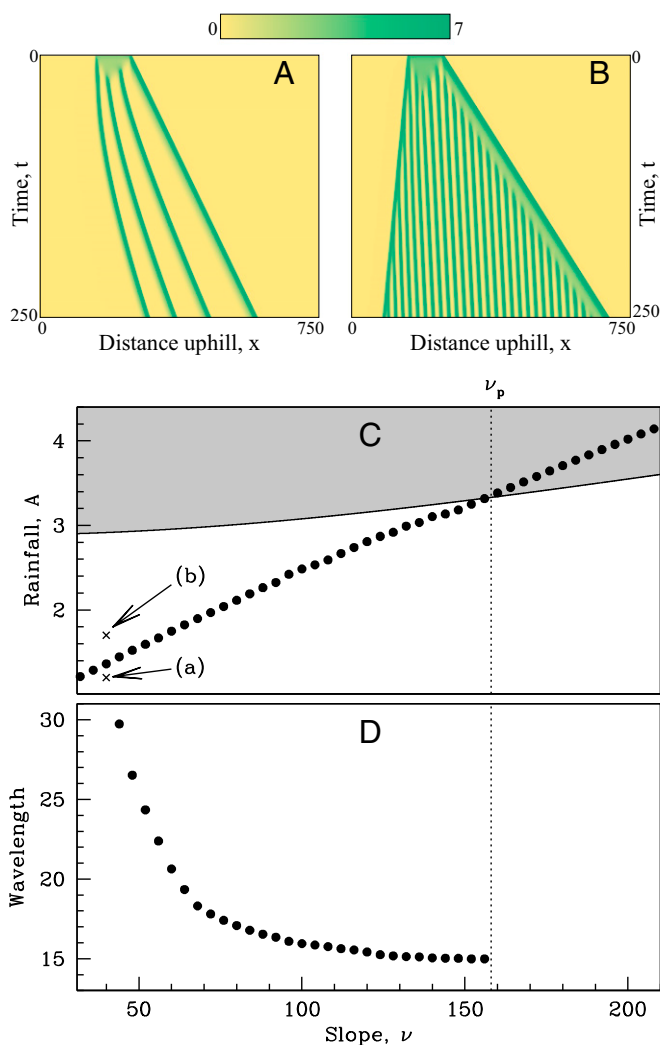


**Fig. 5.** Colonization of bare ground gives an inverse relationship between pattern wavelength and slope. (A) At a rainfall level below the critical level for colonization, both uphill and downhill edges of a vegetation patch move uphill, whereas (B) above the critical level the downhill edge moves downhill. (C) The critical rainfall level above which colonization occurs (dots). The shaded region is that in which vegetation patterns form, so that above  $\nu = \nu_p$  colonization generates uniform vegetation. The crosses indicate the parameter values used in the simulations in A and B. (D) The wavelength of patterns generated by colonization for  $\nu < \nu_p$ . Parameters: (A–D)  $B = 0.45$ ,  $D = 500$ ; (A)  $A = 1.2$ ,  $\nu = 40$ ; (B)  $A = 1.7$ ,  $\nu = 40$ . The colors in A and B indicate vegetation biomass  $u$  as shown in the scale bar.

Fig. 5C shows a typical plot of the rainfall threshold for colonization against slope. The shaded region is where the uniformly vegetated state is stable, so that vegetation does not form bands. On sufficiently steep slopes, say,  $\nu > \nu_p$ , colonization requires a rainfall level in this region. However, for shallower slopes ( $\nu < \nu_p$ ) colonization leads to patterns (Figs. 5A and B and 6). I calculated the wavelength of these patterns in simulations, and found that throughout parameter space it is negatively correlated with slope (Fig. 5D). This predicted wavelength–slope relationship is consistent with empirical data (5, 8–11).

## Discussion

To provide a specific example of the implications of my results, I consider the African Sahel, which is the transition zone between the Sahara and the Sudanian Savanna. Here banded vegetation occurs for slope gradients of about 0.2–1% (6, 7, 10), and parameter estimates place these shallow slopes well below both of

the critical values  $\nu_m$  and  $\nu_p$  (14, 20). My results therefore suggest that wavelength would increase with slope for patterns arising from the degradation of uniform vegetation, and would decrease with slope following the colonization of bare ground. Because there is now a large amount of data indicating the latter trend (8–10), I infer that the banded vegetation in this region has developed via colonization of bare ground—at least in the locations providing the data, which are very widespread.

This inference must be considered in conjunction with historical climate data. Rain gauge records for the Sahel are very limited before about 1920 (47), but there is considerable proxy data for the last five centuries (48–50). This shows that humid conditions prevailed in the Sahel during the 16th and 17th centuries. Evidence for this comes from three independent source types. Most quantitative are fluctuations of lake levels: for example between 1650 and 1700, Lake Chad was 4 m higher than at present (51). Secondly, historical chronologies such as those of the Bornu Empire describe prosperous conditions with famine being very rare (ref. 52, chap. 2). Thirdly, geographical descriptions by European travelers include reports of local peoples retaining memories of markedly more humid conditions (e.g., ref. 51, p. 223). Note that studies of Lake Bosumtwi in Ghana (53) suggest that during the same period (16th and 17th centuries) there was a severe drought near the Guinea Coast, south of the Sahel. This study has been incorrectly described as referring to the Sahel in a number of popular science articles, including (at the time of writing) the Wikipedia page on the Sahel.

The approximate nature of these historical rainfall estimates makes definitive conclusions impossible. However, the humid climate of the 16th and 17th centuries makes it very likely that uniform vegetation was present in areas currently exhibiting patterns. Because I have concluded that vegetation will then have subsequently died out, one can expect such an event to have occurred during the most severe subsequent drought. This occurred c. 1738–1756, and devastated much of the Sahel (48, 50, 53); for example, the resulting famine is reported to have killed half the population of Tombouctou (48, 50, 54).

A central concept in the understanding of desertification is the bistability between vegetated states and desert (15, 16, 55). As

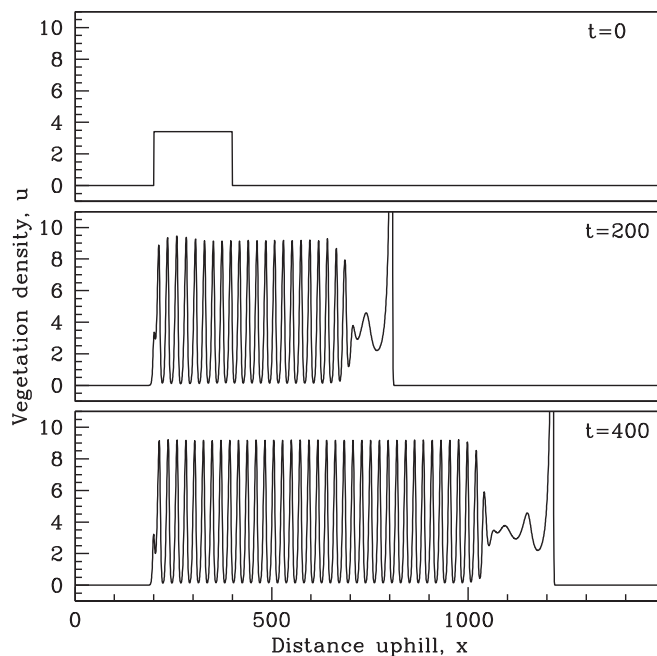


**Fig. 6.** Pattern generation at the smallest rainfall level for colonization of bare ground. Fixing rainfall  $A$  at this critical level  $A_c$  causes the left-hand edge of the vegetation patch to be stationary. Parameters:  $B = 0.45$ ,  $\nu = 56$ ,  $D = 500$ , which imply  $A_c = 1.67$ .

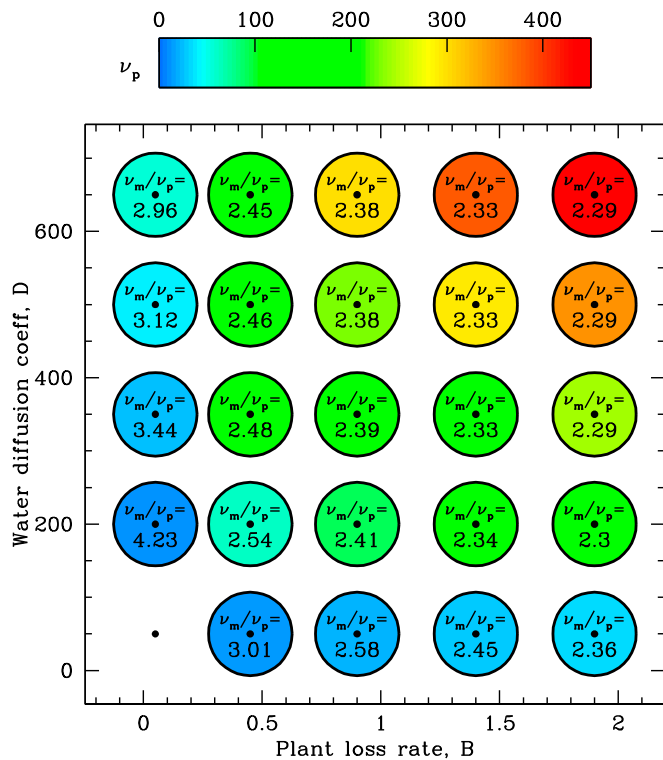


**Fig. 7.** Illustration of when colonization of bare ground results in banded rather than uniform vegetation. This occurs when the slope  $\nu$  is below  $\nu_p$ , whose value is indicated by the colored circles. The wavelength of these bands is always negatively correlated with slope (see Fig. 5D for a typical result). Inside the circles I give the value of  $\nu_m/\nu_p$ , showing that this always exceeds 1; this implies that whenever parameters are such that colonization generates patterned, the degradation of uniform vegetation generates patterns whose wavelength is positively correlated with slope. For  $B=0.05$  and  $D=50$ , colonization generates uniform vegetation for all slopes  $\nu \geq 0$ , and also degradation of bare ground always gives a negative correlation between wavelength and slope, so that neither  $\nu_p$  or  $\nu_m$  is defined; however, these values of  $B$  and  $D$  are significantly outside typical estimates of parameter ranges.

rainfall is decreased, a loss in stability of a vegetated state causes a sudden transition to desert, but if rainfall is subsequently increased back above the tipping point the desert state remains, and reestablishment of vegetation requires much wetter conditions (3, 56, 57). This is reflected in my finding that the critical rainfall level for recolonization is much greater than that required for vegetation survival. For the Sahel, vegetation lost during the drought of c. 1738–1756 may have become reestablished during c. 1760–1790, which was relatively humid with some evidence of appreciable flooding (50). If not, bistability implies that reestablishment would not have occurred until the next markedly humid period, which began in the mid-1800s, following an extended arid interval which began c. 1790 and included a notable drought c. 1828–1839 (47, 50). This suggests that today’s banded vegetation originated by colonization of bare ground either during c. 1760–1790, or since c. 1850. Although there are no empirical data against which this conclusion can be tested directly, it is consistent with the occurrence of localized environmental degradation in the Sahel during the last millennium, for example dune reactivations in Mali which are revealed by optically stimulated luminescence (58).

Even before the current era of satellite images, remote sensing of banded vegetation wavelengths was possible via aerial photography. However, measurement of the corresponding slope gradients required laborious ground-based work, and consequently older data on wavelength–slope relationships are limited. Modern elevation databases eliminate the need for in situ

field work. Thus, remotely sensed wavelength data can easily be complemented by slope gradients. My results indicate that such combined data are far more valuable than wavelength data alone, because they may enable one to infer the historical origin of the vegetation patterns.

## Methods

**Calculation of the Most Unstable Mode.** When  $A \geq 2B$  the model [1] has two homogeneous vegetated steady states; one is always unstable, but

$$u = u_s \equiv \frac{A + \sqrt{A^2 - 4B^2}}{2B} \quad w = w_s \equiv \frac{2B^2}{A + \sqrt{A^2 - 4B^2}}$$

is stable to homogeneous perturbations provided that  $B < 2$ . This restriction on  $B$  holds for all previous parameter estimates (14, 20); for larger  $B$  [1] can have oscillatory dynamics which are never observed in reality. To determine linear stability of  $(u_s, w_s)$  I substitute  $(u, w) = (u_s, w_s) + (\tilde{u}, \tilde{w})e^{i\mathbf{k}\cdot\mathbf{x}}$ ; the spatial frequency of the perturbation is  $k/2\pi$ . Linearizing in  $(\tilde{u}, \tilde{w})$  and requiring nontrivial solutions gives a quadratic for  $\lambda$  with complex coefficients, whose solution yields an explicit formula for the growth rate  $\text{Re } \lambda$  as a function of  $k$ . This formula is a small extension of previous work (12, 32). To determine the most unstable mode I calculated  $\text{Re } \lambda$  over a grid of  $k$  values to give an initial approximation, and then used a numerical nonlinear equation solver to refine this as a solution of  $(d/dk)\text{Re } \lambda = 0$ .

To investigate the correlation between the slope and the wavelength ( $=2\pi/k$ ) of the most unstable mode, I considered the parameter ranges  $0.05 \leq A \leq 5$ ,  $0.025 \leq B \leq 1.975$ ,  $5 \leq \nu \leq 300$ , and  $10 \leq D \leq 800$ , which are chosen to comfortably include all reasonable estimates (14, 20, 23). I considered 100 equally spaced values spanning each of these ranges, giving a total of  $10^8$  parameter sets. Some of these do not satisfy the constraint  $A \geq 2B$ , and for some others the most unstable mode is actually stable. For the remainder (about half) I calculated the change in the frequency of the most unstable mode following small changes in  $A$  and  $\nu$ . In every case, frequency increases with  $A$  and decreases with  $\nu$ .

**Calculation of  $\nu_m$ .** As rainfall  $A$  is decreased, the stability of  $(u_s, w_s)$  changes at a Turing–Hopf bifurcation point,  $A = A_{TH}$ , say. For  $\nu = 0$ , calculation of  $A_{TH}$  reduces to that of a standard Turing bifurcation point for reaction–diffusion equations (32, 59). From this starting point, I numerically continued  $A_{TH}$  and the corresponding spatial frequency as solutions of  $\text{Re } \lambda = (d/dk)\text{Re } \lambda = 0$ , while increasing  $\nu$ . I performed this procedure for the same 100 values of  $B$  and  $D$  as used above ( $10^4$  cases in total). For small  $D$  there is no Turing bifurcation when  $\nu = 0$ : Specifically this occurs when  $(u_s, w_s)$  is stable for  $\nu = 0$  and  $A = 2B$ , the condition for which is  $BD < 2$ . This corresponds to no vegetation patterns forming on flat ground. In fact, such patterning is common, although in the absence of spatial organization by a slope one sees labyrinthine or spotted patterns rather than bands (1, 10). Therefore, these unrealistic parameter sets (0.25% of the total) can be discounted, although for completeness I comment that patterns then exist only for  $\nu$  above a nonzero value, and pattern wavelength decreases with  $\nu$ . When  $BD$  is slightly greater than 2 (about 0.7% of cases) pattern wavelength is also a decreasing function of  $\nu$ . These cases will also not be relevant in applications because the rainfall range giving patterns on flat ground is so small. In all of the remaining cases (about 99%) pattern wavelength increases with  $\nu$  when this is small, reaches a maximum at  $\nu = \nu_m$ , and then decreases (Fig. 3B). I calculated  $\nu_m$  by quadratic interpolation on my grid of  $\nu$  values. Fig. 4 shows  $\nu_m$  as a function of  $B$  and  $D$ . Typical estimates for the value of  $\nu$  corresponding to slopes on which banded vegetation occurs are less than 200 (14, 20), whereas most estimates for  $D$  are at least 500 (21, 23). Therefore, Fig. 4 suggests that a negative correlation between wavelength and slope is restricted to unrealistic parameter values, for patterns arising from degradation of uniform vegetation.

**Investigation of Pattern Generation by Colonization of Bare Ground.** The critical rainfall level above which colonization of bare ground occurs is determined by the change in movement direction of the lower edge of a vegetation patch, from uphill to downhill; in the physics literature this type of transition is known as a “Maxwell point.” I ran model simulations with initial vegetation density set to  $u_s$  in the right-hand (uphill) half of the domain and zero in the left-hand half, with corresponding Dirichlet boundary conditions. After initial transients have dissipated, a transition front develops, moving with a constant speed that is positive (negative) for smaller (larger) values of  $A$ . Using a nonlinear equation solver, I calculated the value  $A = A_c$  at which the speed is zero: this is the threshold rainfall level for colonization. A guide to the appropriate range of  $A$  values to consider is provided by the special case

$\nu = D = 0$ , for which it is possible to obtain exact solutions of the ordinary differential equations satisfied by a stationary transition front, and hence of  $A_c$  (60).

I then calculated the wavelength generated by colonization when  $A = A_c$ . When rainfall slowly increases, this will be the wavelength of the first patterns to be established, which will then persist following further moderate changes in rainfall (19, 23, 38). My procedure was to solve [1] numerically with  $A = A_c$  and with  $u$  set to  $u_s$  in the center of the domain (in a region of width arbitrarily chosen to be 200), and zero otherwise. Fig. 6 shows a typical example of the resulting solution. The left-hand (downhill) edge of the vegetated region remains stationary because  $A = A_c$ , whereas the right-hand edge propagates uphill. The resulting vegetated region can be either uniform or patterned. The division between these cases is illustrated by plotting  $A_c$  against  $\nu$ , and superimposing the  $\nu$ - $A$  parameter regions in which patterns do–do not form; calculation of these regions is described above. Fig. 5C shows one such plot: Patterns develop when the slope  $\nu$  is below a threshold  $\nu_p$ , and Fig. 5D shows that their wavelength decreases with slope. These

figures are typical except that for small values of  $D$  colonization always generates uniform vegetation rather than patterns. For example, when  $B = 0.45$  this occurs for  $D$  less than about 10.

The procedure outlined above is quite expensive in computer time, making it unfeasible to loop over a fine grid of  $B$  and  $D$  values. Instead I considered 25  $B$ - $D$  pairs:  $B = 0.05, 0.45, 0.9, 1.4, 1.9$  and  $D = 50, 200, 350, 500, 650$ . The slight nonuniformity in the spacing of the  $B$  values is deliberate to include 0.45, which is the most commonly used value in other studies using [1]. Fig. 7 shows the dependence on  $B$  and  $D$  of  $\nu_p$ , and also of the ratio  $\nu_m/\nu_p$ . Note that this ratio is always greater than 1, implying that whenever colonization generates patterns, degradation of uniform vegetation with the same parameters would give patterns whose wavelength increases with slope.

**ACKNOWLEDGMENTS.** I thank Professor S. E. Nicholson (Florida State University) for helpful advice, and Professor A. R. White (Heriot-Watt University) and Dr. P. L. Wiener (University of Edinburgh) for careful reading of the manuscript.

- Deblauwe V, Barbier N, Couteron P, Lejeune O, Bogaert J (2008) The global biogeography of semi-arid periodic vegetation patterns. *Glob Ecol Biogeogr* 17(6):715–723.
- Bel G, Hagberg A, Meron E (2012) Gradual regime shifts in spatially extended ecosystems. *Theor Ecol* 5(4):591–604.
- Kéfi S, Rietkerk M, van Baalen M, Loreau M (2007) Local facilitation, bistability and transitions in arid ecosystems. *Theor Popul Biol* 71(3):367–379.
- Lefever R, Barbier N, Couteron P, Lejeune O (2009) Deeply gapped vegetation patterns: On crown/root allometry, criticality and desertification. *J Theor Biol* 261(2):194–209.
- Pelletier JD, et al. (2012) How do vegetation bands form in dry lands? Insights from numerical modeling and field studies in southern Nevada, USA. *J Geophys Res* 117:F04026.
- Valentin C, d'Herbès JM, Poesen J (1999) Soil and water components of banded vegetation patterns. *Catena* 37(1):1–24.
- Deblauwe V, Couteron P, Bogaert J, Barbier N (2012) Determinants and dynamics of banded vegetation pattern migration in arid climates. *Ecol Monogr* 82:3–21.
- Eddy J, Humphreys GS, Hart DM, Mitchell PB, Fanning PC (1999) Vegetation arcs and litter dams: Similarities and differences. *Catena* 37(1):57–73.
- d'Herbès JM, Valentin C, Thiery JM (1997) La brousse tigrée au Niger: Synthèse des connaissances acquises. Hypothèses sur la genèse et les facteurs déterminant les différentes structures contractées. *Fonctionnement et Gestion des Écosystèmes Forestiers Contractés Sahéliens*, eds d'Herbès JM, Ambouta JMK, Peltier R (John Libbey Eurotext, Paris), pp 120–131.
- Deblauwe V, Couteron P, Lejeune O, Bogaert J, Barbier N (2011) Environmental modulation of self-organized periodic vegetation patterns in Sudan. *Ecography* 34(6):990–1001.
- Penny GG, Daniels KE, Thompson SE (2013) Local properties of patterned vegetation: Quantifying endogenous and exogenous effects. *Phil Trans R Soc A* 371:20120359.
- Sherratt JA (2005) An analysis of vegetation stripe formation in semi-arid landscapes. *J Math Biol* 51(2):183–197.
- Stewart J, et al. (2014) Modeling emergent patterns of dynamic desert ecosystems. *Ecol Monogr* 84(3):373–410.
- Klausmeier CA (1999) Regular and irregular patterns in semiarid vegetation. *Science* 284(5421):1826–1828.
- Rietkerk M, et al. (2002) Self-organization of vegetation in arid ecosystems. *Am Nat* 160(4):524–530.
- Gilad E, von Hardenberg J, Provenzale A, Shachak M, Meron E (2007) A mathematical model of plants as ecosystem engineers. *J Theor Biol* 244(4):680–691.
- Barbier N, Couteron P, Lefever R, Deblauwe V, Lejeune O (2008) Spatial decoupling of facilitation and competition at the origin of gapped vegetation patterns. *Ecology* 89(6):1521–1531.
- von Hardenberg J, Kletter AY, Yizhaq H, Nathan J, Meron E (2010) Periodic versus scale-free patterns in dryland vegetation. *Proc R Soc B* 277(1688):1771–1776.
- Sherratt JA (2013) History-dependent patterns of whole ecosystems. *Ecol Complex* 14:8–20.
- Ursino N (2005) The influence of soil properties on the formation of unstable vegetation patterns on hillsides of semiarid catchments. *Adv Water Resour* 28:956–963.
- Kealy BJ, Wolkind DJ (2012) A nonlinear stability analysis of vegetative Turing pattern formation for an interaction-diffusion plant-surface water model system in an arid flat environment. *Bull Math Biol* 74(4):803–833.
- Zelnik YR, Kinast S, Yizhaq H, Bel G, Meron E (2013) Regime shifts in models of dryland vegetation. *Phil Trans R Soc A* 371:20120358.
- Siteur K, et al. (2014) Beyond Turing: The response of patterned ecosystems to environmental change. *Ecol Complex* 20:81–96.
- Callaway RM (1995) Positive interactions among plants. *Bot Rev* 61(4):306–349.
- Rietkerk M, Ketner P, Burger J, Hoorens B, Olf H (2000) Multiscale soil and vegetation patchiness along a gradient of herbivore impact in a semi-arid grazing system in West Africa. *Plant Ecol* 148:207–224.
- Galle S, Ehrmann M, Peugeot C (1999) Water balance in a banded vegetation pattern: A case study of tiger bush in western Niger. *Catena* 37(1):197–216.
- Archer NAL, Quinton JN, Hess TM (2012) Patch vegetation and water redistribution above and below ground in south-east Spain. *Ecohydrology* 5(1):108–120.
- Istanbulluoglu E, Bras RL (2006) On the dynamics of soil moisture, vegetation, and erosion: Implications of climate variability and change. *Water Resour Res* 42:W06418.
- Siteur K, et al. (2014) How will increases in rainfall intensity affect semiarid ecosystems? *Water Resour Res* 50:5980–6001.
- Pueyo Y, Kéfi S, Alados CL, Rietkerk M (2008) Dispersal strategies and spatial organization of vegetation in arid ecosystems. *Oikos* 117(10):1522–1532.
- Baudena M, Rietkerk M (2013) Complexity and coexistence in a simple spatial model for arid savanna ecosystems. *Theor Ecol* 6(2):131–141.
- van der Stelt S, Doelman A, Hek G, Rademacher JDM (2013) Rise and fall of periodic patterns for a generalized Klausmeier-Gray-Scott model. *J Nonlinear Sci* 23:39–95.
- Mou C, et al. (2011) Cryptic patterning of avian skin confers a developmental facility for loss of neck feathering. *PLoS Biol* 9(3):e1001028.
- Barras I, Crampin EJ, Maini PK (2006) Mode transitions in a model reaction-diffusion system driven by domain growth and noise. *Bull Math Biol* 68(5):981–995.
- Barbier N, Couteron P, Lejoly J, Deblauwe V, Lejeune O (2006) Self-organized vegetation patterning as a fingerprint of climate and human impact on semi-arid ecosystems. *J Ecol* 94(3):537–547.
- Kusserow H, Haenisch H (1999) Monitoring the dynamics of “tiger bush” (brousse tigrée) in the West African Sahel (Niger) by a combination of Landsat MSS and TM, SPOT, aerial and kite photographs. *Photogramm Fernerkund Geoinf* 2:77–94.
- Sherratt JA, Lord GJ (2007) Nonlinear dynamics and pattern bifurcations in a model for vegetation stripes in semi-arid environments. *Theor Popul Biol* 71(1):1–11.
- Dagbovie AS, Sherratt JA (2014) Pattern selection and hysteresis in the Rietkerk model for banded vegetation in semi-arid environments. *J R Soc Interface* 11(99):20140465.
- Tsai JC, Sneyd J (2005) Existence and stability of traveling waves in buffered systems. *SIAM J Appl Math* 66:237–265.
- Alzahrani EO, Davidson FA, Dodds N (2012) Reversing invasion in bistable systems. *J Math Biol* 65(6–7):1101–1124.
- Sneyd J, Keener J (2009) *Mathematical Physiology* (Springer, New York).
- Fife PC, McLeod JB (1977) The approach of solutions of nonlinear diffusion equations to travelling front solutions. *Arch Ration Mech Anal* 65(4):335–361.
- Dockery JD, Lui R (1994) Existence and stability of traveling wave solutions for a population genetic model via singular perturbations. *SIAM J Appl Math* 54:231–248.
- Montaña C, Seghieri J, Cornet A (2001) Vegetation dynamics: Recruitment, regeneration in two-phase mosaics. *Banded Vegetation Patterning in Arid and Semi-Arid Environments*, eds Tongway DJ, Valentin C, Seghieri J (Springer, New York), pp 132–145.
- Tongway DJ, Ludwig JA (2001) Theories on the origins, maintenance, dynamics, and functioning of banded landscapes. *Banded Vegetation Patterning in Arid and Semi-Arid Environments*, eds Tongway DJ, Valentin C, Seghieri J (Springer, New York), pp 20–31.
- Wu XB, Thurow TL, Whisenant SG (2000) Fragmentation and changes in hydrologic function of tiger bush landscapes, south-west Niger. *J Ecol* 88(5):790–800.
- Nicholson SE, Dezfuli AK, Klotter D (2012) A two-century precipitation dataset for the continent of Africa. *Bull Am Meteorol Soc* 93(8):1219–1231.
- Nicholson SE (1978) Climatic variations in the Sahel and other African regions during the past five centuries. *J Arid Environ* 1(1):3–24.
- Nicholson SE (1979) The methodology of historical climate reconstruction and its application to Africa. *J Afr Hist* 20:31–49.
- Nicholson SE (1980) Saharan climates in historic times. *The Sahara and the Nile: Quaternary Environments and Prehistoric Occupation in Northern Africa*, eds Williams MAJ, Fuere H (Balkema, Rotterdam), pp 173–200.
- Maley J (1973) Mécanisme des changements climatiques aux basses latitudes. *Palaeogeogr Palaeoclimatol Palaeoecol* 14:193–227.
- Gado BA (1993) *Une Histoire des Famines au Sahel* (L'Harmattan, Paris).
- Shanahan TM, et al. (2009) Atlantic forcing of persistent drought in West Africa. *Science* 324(5925):377–380.
- Iliffe J (2007) *Africans: The History of a Continent* (Cambridge Univ Press, Cambridge, UK).
- Kéfi S, Eppinga MB, de Ruiter PC, Rietkerk M (2010) Bistability and regular spatial patterns in arid ecosystems. *Theor Ecol* 3(4):257–269.
- Meron E (2012) Pattern-formation approach to modelling spatially extended ecosystems. *Ecol Modell* 234:70–82.
- Scheffer M, Carpenter S, Foley JA, Folke C, Walker B (2001) Catastrophic shifts in ecosystems. *Nature* 413(6856):591–596.
- Stokes S, Bailey RM, Fedoroff N, O'Marah KE (2004) Optical dating of aeolian dynamics on the West African Sahelian margin. *Geomorphology* 59(1):281–291.
- Murray JD (2003) *Mathematical Biology II: Spatial Models and Biomedical Applications* (Springer, New York).
- Sherratt JA, Synodinos AD (2012) Vegetation patterns and desertification waves in semi-arid environments: Mathematical models based on local facilitation in plants. *Discrete Cont Dyn Syst Ser B* 17:2815–2827.